# Frequency locking, quasiperiodicity, and chaos in dual-frequency loss-modulated erbium-doped fiber lasers

**Yue Liu (刘 越)*, Wei Zhang (张 巍), Xue Feng (冯 雪), and Xiaoming Liu (刘小明)**

*Department of Electronic Engineering, Tsinghua University, Beijing 100084, China*

**E-mail: liuyue02@mails.thu.edu.cn*

Received October 30, 2008

Dynamic behaviors of the erbium-doped fiber laser (EDFL) with dual-frequency loss modulation are experimentally investigated. Frequency-locked states with their winding numbers which form the devil's staircase are observed in this kind of lasers. In the unlocked regions, the output state changes from quasiperiodicity to chaos under increasing modulation index, which demonstrates a different route to chaos from the conventional loss-modulated EDFLs with a single modulation frequency. The chaos output in the dual-frequency loss-modulated EDFLs shows less harmonic components of the modulation frequency in the corresponding power spectrum, indicating the improvement of the randomness of the chaotic signals.

*OCIS codes:* 140.1540, 140.3500.

*doi: 10.3788/COL20090708.0699.*

Chaos in erbium-doped fiber lasers (EDFLs) has attracted much attention because of its potential applications in secure optical communication[1−3]. It has been demonstrated and investigated intensively that complex dynamic behaviors can be realized by EDFLs by using heavily doped EDF with high ion pair concentration[4−6]. On the other hand, chaos generation by introducing additional degrees of freedom[7], e.g., the loss modulation[8], focused much attention in recent years since common EDFs can be used in these EDFLs, which improves their practicality[9].

Recently, chaos synchronization has been demonstrated in loss-modulated EDFLs[1,9]. However, due to the single-frequency modulation used in these works, the randomness of the chaos output is limited, which is reflected by the obvious components at the modulation frequency and its harmonics in the chaotic power spectra[1]. Therefore, the EDFLs with more additional loss modulation need to be investigated.

In this letter, we propose and demonstrate that dual-frequency loss modulation (driving) can be used as additional freedom degrees of EDFLs. The dynamical behaviors of the dual-frequency loss-modulated EDFL are investigated experimentally. The phenomena of frequency locking and chaos via quasiperiodicity are observed. These fiber lasers show their potential as chaos generators with better randomness in comparison with the ones with single driving frequency by studying the chaotic power spectra.

The experimental setup of the loss-modulated EDFL is shown in Fig. 1. This EDFL is a ring laser. The gain device is an erbium-doped fiber amplifier (EDFA) comprised of a piece of 25-m long EDF (MP980, OFS) pumped by a 980-nm pump-laser and an isolator. In all the experimental results shown below, the pump power is fixed at 56 mW. A band-pass filter composed of a fiber Bragg grating (FBG) and an optical circulator, is inserted into the cavity. The FBG has a reflectivity of 90% at 1546.7 nm and a 3-dB bandwidth of 0.2 nm. The polarization in the cavity is adjusted by a polarization controller (PC). A pair of acousto-optical modulators (AOMs) with the opposite frequency shift (±27 MHz) are used as the loss modulation devices. The external modulation signal (S) is added on AOM1 which shifts the optical frequency from $\nu_0$ to $\nu_0$+27 MHz to realize harmonic modulation of the cavity loss, while AOM2 works in continuous wave (CW) mode to eliminate the self-pulsing caused by the frequency-shifted feedback of the AOM[10]. Their place can be exchanged without affection on the results of the experiments. The signal voltage applied to the AOM driver for the combined modulation is

$$S(t) = V_b[1 + m_1 \sin(2\pi f_1 t) + m_2 \sin(2\pi f_2 t)], \qquad (1)$$

where $V_b$ is the bias voltage and equals 438 mV in our experiments, $m$ ($m = V/V_b$, $V$ is the driving voltage amplitude) and $f$ are the modulation index and the modulation frequency of the two independent sinusoidal signals identified by suffixes $i$ ($i = 1, 2$), respectively. The laser light is divided by a fiber coupler with a coupling ratio of 80:20. The total cavity length is 57 m and the relaxation oscillation frequency of the laser is about 14 kHz. The laser's temporal output is measured by a photodetector (PD, Agilent 83440B) with a bandwidth of 6 GHz and an oscilloscope (OSC, Agilent 54833A) with a bandwidth of 1 GHz. The power spectrum of the temporal output is also analyzed and shown on the screen of the OSC, using the fast Fourier transformation (FFT) function of the OSC.

Firstly, the mearsurement is performed for the EDFL without any modulation and the laser emits in a CW regime in the pump condition. The output trace and its corresponding power spectrum are shown in Figs. 2(a) and (b), respectively. When the loss of the EDFL is modulated by a driving signal at $m_1$=2.6%, the pulses appear [see Fig. 2(c)] and the modulation frequency, $f_1$=43847 Hz, marked by the arrow, is shown in the corresponding

 

power spectrum [see Fig. 2(d)]. The smaller peaks shown in the power spectra are mainly due to the relaxation oscillation of the EDFL. The fact demonstrates that the origin of the pulsed condition cannot be attributed to the noise of the laser but the loss modulation.

Then temporal output states with stable frequency locking are observed in this EDFL with dual-frequency loss modulation. Some typical traces of output signal voltage ($V_{\rm out}$) versus $t$ are shown in Fig. 3. In these traces, the values of the driving frequency ratio $\Omega = f_1/f_2$ have been specially chosen to be 2/5, 1/2, 3/5, and 2/3, respectively. It can be seen that each trace shows a well-defined periodicity. Each stable frequency-locked state can be represented by the corresponding rational winding numbers[11,12] $w = p/q$, where $p$ and $q$ are prime numbers. In Fig. 4, the winding number is shown as a function of the frequency ratio in the interval of [1/3, 1] by sweeping $f_1$ from 1200 Hz to 4000 Hz while $f_2$ is fixed at 4000 Hz. The winding numbers form a fractal curve called a devil's staircase and appear in the Farey-tree order from left to right[13]. The width of the range for the frequency ratio which gives a stable $p/q$ frequency-locked state depends on the level where $p/q$ appears in the hierarchy of the Farey tree. For all experimental results shown in Fig. 3 and Fig. 4, the modulation indices are $m_1 = 2.6\%$ and $m_2 = 3.2\%$, respectively.

The gaps between two stairs are the unlocked regions. Under the modulation indices in Fig. 4, the temporal outputs in the unlocked regions are generally quasiperiodic, reflecting a complex beating of two modulation frequencies. When one of the modulation indices (here $m_1$) increases, a transition from quasiperiodicity to chaos can be observed. Figure 5 shows the transition processes when the modulation frequency ratio $\Omega = f_1/f_2$ ($f_1$ = 2475 Hz and $f_2$ = 4000 Hz) is almost equal to the gold mean $\sigma_{\rm g} = (\sqrt{5}-1)/2$. The chosen value represents the 'worst' irrational number because it is the most difficult one to be approximated by rational numbers[14]. As $m_2 = 3.2\%$, Figs. 5(a), (c), and (e) are temporal output traces under different $m_1$, while Figs. 5(b), (d), and (f) are their corresponding spectra. There are two traces in each figure of Figs. 5(a), (c), and (e), showing the temporal output traces (lower) and details of their pulse series (upper), respectively. As $m_1 = 2.6\%$, the power spectrum [see Fig. 5(b)] displays the components of modulation frequencies ($f_1$ and $f_2$) and their harmonics, as well as various combinations of the modulation frequencies e.g., $f_1 + f_2$, showing its characteristics of quasiperiodicity. When $m_1$ increases to 4.9%, the components of the various modulation frequency combinations are enhanced, and at the same time a broadband noise appears in the power spectrum [see Fig. 5(d)], showing the onset of chaos. When $m_1$ increases to 6.5%, the broadband noise in the power spectrum rises significantly and covers the most combinations components of the modulation frequencies [see Fig. 5(f)], indicating chaos of the laser system.

Figure 6 shows similar experimental results of the transition to chaos via quasiperiodicity when the modulation frequency ratio $\Omega = f_1/f_2$ ($f_1$ = 1656 Hz and $f_2$ = 4000 Hz) is approximately equal to the silver mean

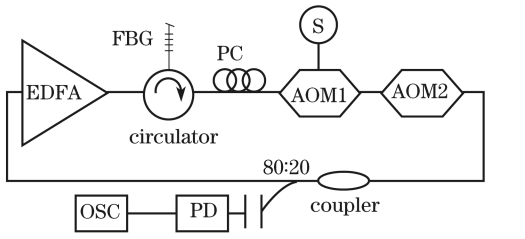


Fig. 1. Experimental setup of the dual-frequency loss-modulated EDFL.

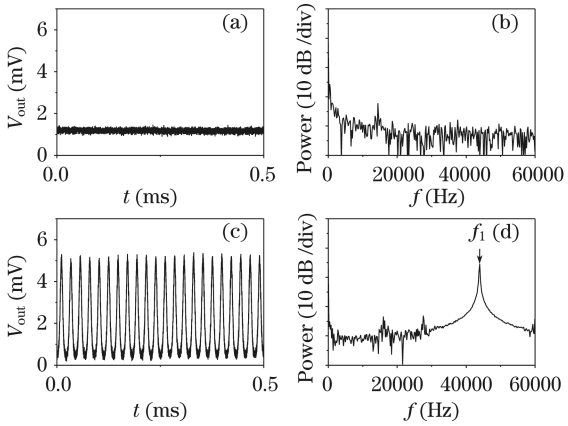


Fig. 2. Output traces and their corresponding power spectra of the EDFL. (a), (b): Without any modulation; (c), (d): with a modulation signal, $f_1$=43847 Hz, $m_1$=2.6%.

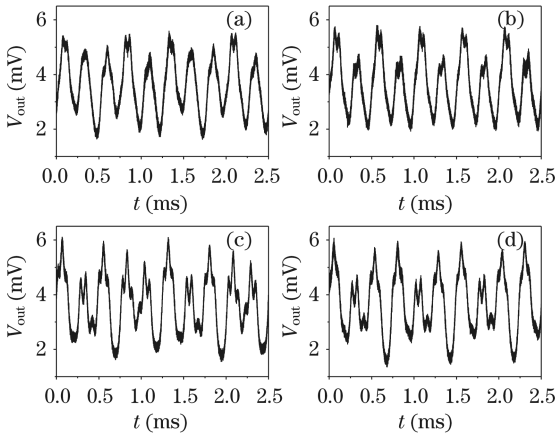


Fig. 3. Typical frequency locking output traces. (a) $f_1$= 1600 Hz, $w$=2/5; (b) $f_1$=2000 Hz, $w$=1/2; (c) $f_1$=2400 Hz, $w$=3/5; (d) $f_1$=2667 Hz, $w$=2/3. Other modulation parameters: $m_1$=2.6%, $f_2$=4000 Hz, $m_2$=3.2%.

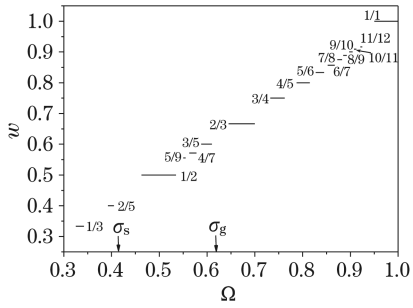


Fig. 4. Measured winding numbers as a function of the frequency ratio $\Omega = f_1/f_2$.

$\sigma_s = \sqrt{2}-1$. However, the modulation index threshold of the transition from quasiperiodicity to chaos at $\Omega = \sigma_s$ is higher than that at $\Omega = \sigma_g$ while other parameters of the laser are same. We find that chaos via quasiperiodicity occurs in each unlocked region shown in Fig. 4 at different transition threshold as the modulation index increases. The lowest threshold is achieved at $\Omega = \sigma_g$ due to the irrational characteristics of the golden mean, indicating that chaos can be achieved more easily under this value of the frequency ratio.

It is well known that the period-doubling and intermittency routes to chaos in EDFLs[15], which are also realized in our experimental setup by adding one driving signal only. Figure 7 shows the comparison between the typical chaotic spectra of loss-modulated EDFLs with single- and dual-frequency modulation. In Fig. 7(a), it is seen that lines occur at the modulation frequency and its harmonics in the chaotic power spectrum of the single-frequency loss-modulated EDFL, which shows that the chaos is not completely random[1]. In Fig. 7(b), the frequency spectrum of the dual-frequency loss-modulated EDFL has better continuity owing to the suppression of the periodic frequency lines. It indicates that chaos in dual-frequency loss-modulated EDFL is more random. Here, the frequency ratio is chosen to be approximately equal to $\sigma_g$.

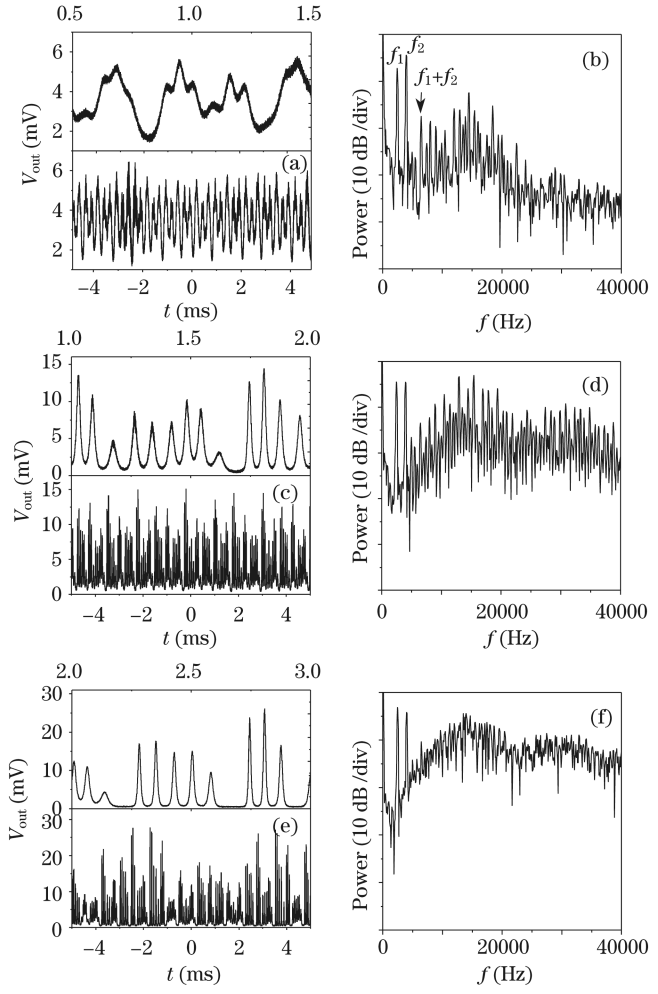


Fig. 5. Transition from quasiperiodicity to chaos at $\Omega \approx \sigma_g$. (a), (b): $m_1$=2.6%, $m_2$=3.2%; (c), (d): $m_1$=4.9%, $m_2$=3.2%; (e), (f): $m_1$= 6.5%, $m_2$=3.2%.

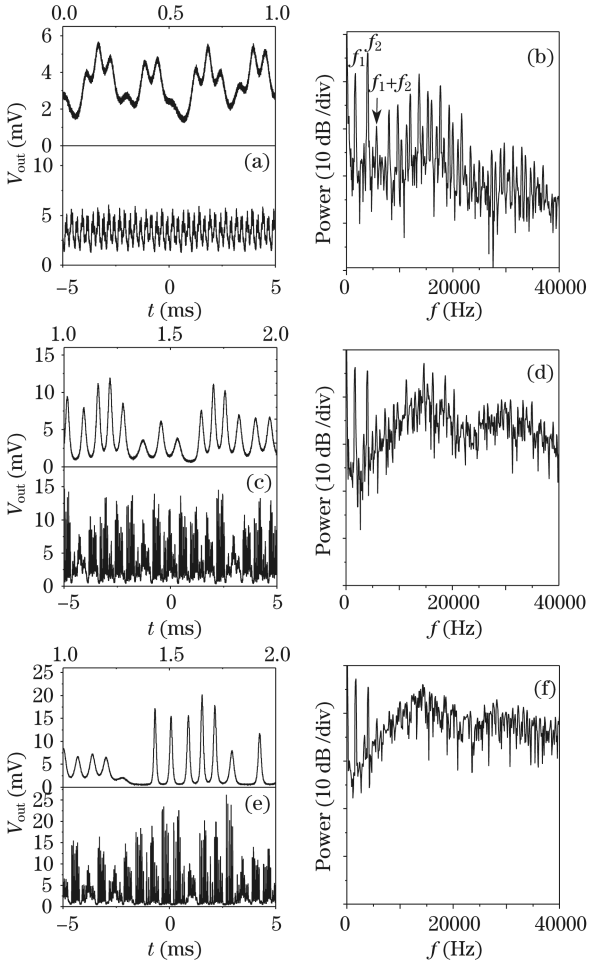


Fig. 6. Transition from quasiperiodicty to chaos at $\Omega \approx \sigma_s$. (a), (b): $m_1$=2.6%, $m_2$=3.2%; (c), (d): $m_1$=8.6%, $m_2$=3.2%; (e), (f): $m_1$= 9.7%, $m_2$=3.2%.

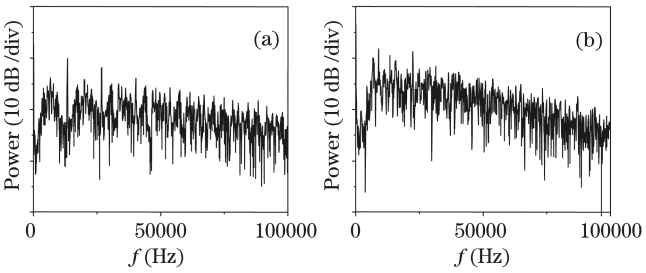


Fig. 7. Comparison of chaotic spectra for two kinds of modulation methods. (a) $f_1$=13400 Hz, $m_1$=2.6%; (b) $f_1$= 13400 Hz, $m_1$=2.6%, $f_2$=22385 Hz, $m_2$=3.2%.

It is worth to note that frequency locking and the transition from quasiperiodicity to chaos caused by competing effect of the natural frequency and the pump modulation frequency has also been observed in a pump-modulated self-pulsing EDFL[16,17], in which heavily doped EDF is required. In this letter, the results demonstrate that by dual-frequency loss-modulation chaos via quasiperiodicity as well as frequency locking can be realized in EDFLs using common EDFs, which extends the practicability of loss-modulated EDFLs in optical secure

communication.

In conclusion, we report the experimental results on the quasiperiodic route to chaos in a dual-frequency loss-modulated EDFL for the first time. Comparing the spectrum with that of the conventional loss-modulated EDFLs with single modulation frequency, we find that the chaos signal in our results is more random because of the absence of the harmonics of the modulation frequencies, indicating the enhancement of the randomness. Frequency-locked states with their winding numbers appearing in the Farey-tree order and forming the devil's staircase are also observed in this kind of lasers.

## References

1. L. Luo and P. Chu, J. Opt. Soc. Am. B **15,** 2524 (1998).
2. L. Yang, W. Pan, B. Luo, W. Zhang, N. Jiang, Z. Zhou, and G. Yang, Chinese J. Lasers (in Chinese) **35,** 992 (2008).
3. S. Yan, Z. Chi, and W. Chen, Acta Opt. Sin. (in Chinese) **24,** 29 (2004).
4. F. Sanchez, M. LeFlohic, G. M. Stephan, P. LeBoudec, and P.-L. Francois, IEEE J. Quantum Electron. **31,** 481 (1995).
5. F. Sanchez and G. Stéphan, Phys. Rev. E **53,** 2110 (1996).
6. P. Besnard, F. Ginovart, P. Le Boudec, F. Sanchez, and G. M. Stéphan, Opt. Commun. **205,** 187 (2002).
7. J. Zhang, G. Li, and Z. Zhang, Chinese J. Lasers (in Chinese) **21,** 540 (1994).
8. J. M. Saucedo-Solorio, A. N. Pisarchik, A. V. Kir'yanov, and V. Aboites, J. Opt. Soc. Am. B **20,** 490 (2003).
9. S. Kim, B. Lee, and D. Kim, IEEE Photon. Technol. Lett. **13,** 290 (2001).
10. J. Maran, P. Besnard, and S. LaRochelle, J. Opt. Soc. Am. B **23,** 1302 (2006).
11. P. Bak, Phys. Today **39,** 38 (1986).
12. D. He, W. J. Yeh, and Y. H. Kao, Phys. Rev. B **30,** 172 (1984).
13. D. Baums, W. Elsässer, and E. O. Göbel, Phys. Rev. Lett. **63,** 155 (1989).
14. H. Winful, Y. Chen, J. Liu, Appl. Phys. Lett. **48,** 616 (1986).
15. L. Luo, T. J. Tee, and P. L. Chu, J. Opt. Soc. Am. B **15,** 972 (1998).
16. A. N. Pisarchik and Y. O. Barmenkov, Opt. Commun. **254,** 128 (2005).
17. A. N. Pisarchik, A. V. Kir'yanov, Y. O. Barmenkov, and R. Jaimes-Reátegui, J. Opt. Soc. Am. B **22,** 2107 (2005).